




Screened extended Koopmans' theorem: Photoemission at weak and strong correlationS. Di Sabatino ^{1,2,*}, J. Koskelo ², J. A. Berger ¹ and P. Romaniello ^{2,†}¹Laboratoire de Chimie et Physique Quantiques, Université de Toulouse, CNRS, UPS and ETSF, F-31062 Toulouse, France²Laboratoire de Physique Théorique, Université de Toulouse, CNRS, UPS and ETSF, F-31062 Toulouse, France

(Received 6 October 2022; accepted 15 December 2022; published 6 January 2023)

By introducing electron screening in the extended Koopmans' theorem we correctly describe the band-gap opening in weakly as well as strongly correlated systems. We show this by applying our method to bulk LiH, Si, and paramagnetic as well as antiferromagnetic NiO. Although incorrect features remain in the full photoemission spectra, this is a remarkable result for an *ab-initio* electronic structure method and it opens the way to a unified description of photoemission spectra at weak and strong correlation.

DOI: [10.1103/PhysRevB.107.035111](https://doi.org/10.1103/PhysRevB.107.035111)**I. INTRODUCTION**

Photoemission spectroscopy is an essential experimental tool to characterize the electronic structure of a system. In particular, it can be used to trace phase transitions, which are especially important in strongly correlated systems. Indeed, one of the most fascinating phenomena characterizing the physics of these systems is undoubtedly the Mott-Hubbard metal-to-insulator transition (MIT) [1]. Here, the appearance of an insulating state is a direct consequence of the strong Coulomb repulsion, rather than of the underlying electronic band structure. Systems at the edge of a metal-to-insulator transition exhibit a wealth of exotic properties owing to their high sensitivity to external parameters (carrier concentration, temperature, external magnetic field), which makes them easy to manipulate. Therefore, in addition to the interesting fundamental physics, possible technological applications are plentiful. Nowadays very accurate and detailed photoemission spectra can be measured.

On the other hand, theory is crucial for the analysis of the experiments as well as the prediction of material properties. In particular, so-called first-principles methods, such as density functional theory (DFT) [2] and many-body perturbation theory (MBPT) based on Green's functions [3], have the potential to be predictive, since no empirical or adjustable parameters are involved. However, standard implementations of these methods are known to work reasonably well for weakly to moderately correlated materials, such as metals and standard semiconductors (e.g., Si or GaAs) [4], but fail for most strongly correlated systems [5]. A paradigmatic example of this kind of materials is paramagnetic NiO, which is predicted to be a metal by standard approximations. This of course sets limits on the description and prediction of metal-to-insulator phase transitions. Going beyond existing approximations is a challenge both from a fundamental [6,7] and a practical point of view [8–10].

We have recently investigated the extended Koopmans' theorem (EKT) [11,12] as a promising method to describe photoemission in solids and, in particular, in strongly correlated systems [5,13–17]. The EKT can be used with any theory that yields the one- and two-body reduced density matrices (1-RDM and 2-RDM, respectively), which are the essential ingredients of this approach [18–21]. For example, the EKT can be used within quantum Monte Carlo (QMC) [18]. However, strongly correlated materials are described by multideterminant wave functions which are difficult to treat in QMC. It is thus desirable to use the EKT together with an approach such as reduced density matrix functional theory (RDMFT) [22–24] that can describe strong correlations. Moreover, within RDMFT the EKT approach is based on a simple matrix diagonalization. However, even with exact density matrices, the EKT tends to overestimate band gaps, with the deviation from experiment increasing with increasing electron correlation. This error is amplified by the use of approximate density matrices [16]. Improvements can be obtained by designing better density matrix approximations, or by going beyond the “quasiparticle ansatz” at the core of the EKT equations, or both. In general, designing new approximate density matrices for solids is a difficult task because most of the available approximations are designed for molecules and their extension to solids is not straightforward.

We have recently proposed to introduce electron screening in standard density matrix approximations available for solids since it is crucially important to describe many-electron systems. For example, in the context of many-body perturbation theory (MBPT) based on Green's functions, the improvement of the *GW* approximation over Hartree-Fock (HF) is precisely owing to the screening of the Coulomb interaction. However, although the inclusion of screening in standard density matrix approximations reduces the gap, its effect is too large, which results in a zero gap in semiconductors and insulators [17] (as an example, the photoemission spectrum (PES) of bulk Si is reported in the Supplemental Material [25]).

Instead, in this paper, we focus on the improvement of the EKT itself by directly including electron screening in the EKT equations. We will show that this approach leads to much

* stefano.disabatino@irsamc.ups-tlse.fr

† pina.romaniello@irsamc.ups-tlse.fr

improved photoemission spectra for both weakly and strongly correlated materials.

II. THEORY

Using the EKT within the basis of natural orbitals (NO), i.e., the orbitals which diagonalize the one-body density matrix, the spectral function, which is related to photoemission spectra, can be written as $A(\omega) = \sum_i [n_i \delta(\omega - \epsilon_i^R) + (1 - n_i) \delta(\omega - \epsilon_i^A)]$, with n_i the occupation number of state i [16]. The removal and addition energies ϵ_i^R and ϵ_i^A , respectively, are given by [26]

$$\epsilon_i^R = h_{ii} + \sum_j V_{ijij} n_j + \frac{1}{n_i} \sum_{jkl} V_{ijkl} \Gamma_{xc,klji}^{(2)}, \quad (1)$$

$$\epsilon_i^A = h_{ii} + \sum_j V_{ijij} n_j - \frac{1}{1 - n_i} \left[\sum_j V_{ijji} n_j - \sum_{jkl} V_{ijkl} \Gamma_{xc,klji}^{(2)} \right], \quad (2)$$

where $h_{ij} = \int d\mathbf{r} \phi_i^*(\mathbf{r}) h(\mathbf{r}) \phi_j(\mathbf{r})$ and $V_{ijkl} = \int d\mathbf{r} d\mathbf{r}' \phi_i^*(\mathbf{r}) \phi_j^*(\mathbf{r}') V(\mathbf{r} - \mathbf{r}') \phi_k(\mathbf{r}) \phi_l(\mathbf{r}')$ are the matrix elements of the single-particle Hamiltonian $h(\mathbf{r}) = -\nabla_{\mathbf{r}}^2/2 + V_{\text{ext}}(\mathbf{r})$, with $V_{\text{ext}}(\mathbf{r})$ the external potential created by atomic nuclei, and the Coulomb interaction $V(\mathbf{r}) = 1/|\mathbf{r}|$, respectively. The 2-RDM is defined as $\Gamma_{klji}^{(2)} = \langle \Psi_0 | c_i^\dagger c_j^\dagger c_l c_k | \Psi_0 \rangle$, where c_i (c_i^\dagger) is the annihilation (creation) operator of an electron in orbital i and $|\Psi_0\rangle$ is the ground-state many-body wave function. The exchange-correlation part of the 2-RDM reads $\Gamma_{xc,klji}^{(2)} = \Gamma_{klji}^{(2)} - n_i n_j \delta_{ik} \delta_{jl}$ and has to be approximated in practice. In this paper we use the power functional (PF) $\Gamma_{xc,klji}^{(2)} = -n_i^\alpha n_j^\alpha \delta_{il} \delta_{jk}$, where $0.5 \leq \alpha \leq 1$. This functional provides an interpolation between the so-called Müller functional [27] ($\alpha = 0.5$), which has a tendency to overcorrelate, and Hartree-Fock ($\alpha = 1$), which neglects correlation. The values suggested in the literature usually vary between 0.55 and 0.7 [28,29]. In most of the works in the literature a value of $\alpha = 0.65$ is used for real solids. Equations (1) and (2), within the PF approximation to Γ_{xc} , give the qualitatively correct picture in correlated solids, but the fundamental band gap is very much overestimated [5,15].

We note that a photoemission experiment could be seen as (at least) a three-particle process, i.e., the photoparticle (electron or hole added to the system), which gives rise to a quasiparticle peak, and the electron-hole pair that it generates by exciting the system, which gives rise to a satellite peak. The EKT is designed to capture quasiparticle peaks in the photoemission spectra but not satellites because it only explicitly considers one-hole and one-electron excitations. However, the EKT can be generalized to two electrons–one hole and two holes–one electron excitations (EKT-3) to also describe satellites. The explicit inclusion of electron-hole excitations can also improve the quasiparticle energies as these excitations capture part of the screening of the added hole or electron [19]. The EKT-3 is similar in spirit to the use of the three-particle Green's function (instead of the one-particle Green's function) to describe photoemission, since it treats on equal footing quasiparticles and satellites [30]. However, an

important drawback of the EKT-3 approach is that it yields equations that depend also on the three- and four-body density matrices (3-RDM and 4-RDM, respectively), which makes EKT-3 computationally very expensive. Moreover, it requires practical approximations to the 3-RDM and 4-RDM, which are not available for solids. In this paper we include the effect of the electron-hole pairs in the EKT equations in an effective way through the screening. Here, we achieve this in a similar way as one can obtain the *GW* approximation from the HF approximation, i.e., we replace the bare Coulomb potential in the exchange-correlation part of the EKT equations by the (statically) screened Coulomb potential. This leads to the screened extended Koopmans' theorem (SEKT). The SEKT equations are thus given by

$$\epsilon_i^R = h_{ii} + \sum_j V_{ijij} n_j + \frac{1}{n_i} \sum_{jkl} W_{ijkl} \Gamma_{xc,klji}^{(2)}, \quad (3)$$

$$\epsilon_i^A = h_{ii} + \sum_j V_{ijij} n_j - \frac{1}{1 - n_i} \left[\sum_j W_{ijji} n_j - \sum_{jkl} W_{ijkl} \Gamma_{xc,klji}^{(2)} \right], \quad (4)$$

where $W = \varepsilon^{-1}V$ is the statically screened Coulomb interaction, with ε the dielectric function. The SEKT is further motivated by the following two arguments: (i) A general screening of the form $W_{ijkl} = \beta_i V_{ijkl}$ ($0 < \beta_i < 1$) can reproduce some of the effects of higher-order RDMs [5]; (ii) Eqs. (3) and (4) reduce to the screened exchange (SEX) equations of MBPT for single Slater determinants. In this case, indeed, the exchange-correlation part of the 2-RDM can be factorized as $\Gamma_{xc,klji}^{(2)} = -n_i n_j \delta_{il} \delta_{jk}$ with the natural occupation numbers n_i being zero or one, and this results in $\epsilon_i^R = \epsilon_i^A = h_{ii} + \sum_j V_{ijij} n_j - \sum_{jkl} W_{ijji} n_j$, which correspond to the poles of the one-body Green's function obtained using the (static) screened exchange self-energy. It therefore becomes clear that, with the power functional approximation to the 2-RDM, Eqs. (3) and (4) tend to the SEX energy equations for weakly correlated systems, which are characterized by occupation numbers close to zero or one. We will now show that the SEKT, besides describing correctly the PES of weakly correlated systems, can reproduce reasonably good PES (although some important deviations remain) for strongly correlated systems, which are characterized by highly fractional natural occupation numbers.

III. RESULTS

We have implemented the EKT and SEKT equations in a modified version of the full-potential linearized augmented plane-wave code ELK [28,31]. In order to build the screened Coulomb exchange matrix elements W_{ijji} we first calculate the static screening matrix in reciprocal space using the random-phase approximation (RPA); the matrix elements in the NO basis are then obtained as

$$W_{ijji} = \frac{1}{\Omega N_q} \sum_{\mathbf{q}\mathbf{G}\mathbf{G}'} W_{\mathbf{G}\mathbf{G}'}(\mathbf{q}) \langle j | e^{-i(\mathbf{q}+\mathbf{G})\cdot\mathbf{r}} | i \rangle^* \times \langle j | e^{-i(\mathbf{q}+\mathbf{G}')\cdot\mathbf{r}} | i \rangle \delta_{\mathbf{q},\mathbf{k}_i - \mathbf{k}_j}, \quad (5)$$

where $i = (\tilde{i}, \mathbf{k}_i)$ is a generalized index that comprises the band index \tilde{i} and the wave vector \mathbf{k}_i , Ω and N_q are the unit cell volume and the number of points in the Brillouin zone sampling, \mathbf{G} is a reciprocal lattice vector, \mathbf{q} is a vector that belongs to the first Brillouin zone, $W_{\mathbf{G},\mathbf{G}'}(\mathbf{q})$ is the Fourier transform of the statically screened Coulomb interaction $W(\mathbf{r}, \mathbf{r}')$, and the oscillator strengths are

$$\langle i | e^{-i(\mathbf{q}+\mathbf{G})\cdot\mathbf{r}} | j \rangle = \int d\mathbf{r} \phi_i^*(\mathbf{r}) e^{-i(\mathbf{q}+\mathbf{G})\cdot\mathbf{r}} \phi_j(\mathbf{r}).$$

The plane-wave cutoff G_{\max} is chosen by requiring $rG_{\max} = 10$ a.u., where r is the muffin-tin radius. More details about the protocol used for the calculations can be found in Ref. [16].

We apply our method to two classes of systems: bulk LiH and Si as examples of weakly correlated systems, and paramagnetic (PM) and antiferromagnetic (AFM) NiO as examples of strongly correlated systems. We note that the paramagnetic phase is modeled as nonmagnetic (NM), therefore in the following, paramagnetic NiO will be referred to as NM NiO.

In principle one could use a self-consistent procedure to calculate the RPA screening, as it is done in, for example, eigenvalue self-consistent GW . However, this can be computationally expensive. Therefore, in this work we adopt a strategy similar to one-shot GW , in which the self-energy is calculated only once with the best G and best W available. For the simple semiconductors, LiH and Si, we use the local-density approximation (LDA) energies and wave functions to calculate the random-phase approximation (RPA) screening. For AFM NiO the LDA band gap is too small. The Heyd-Scuseria-Ernzerhof (HSE03) [32] functional has been proven to be more suitable for this system [33]. Since HSE03 and LDA+ U band structures are very similar for AFM NiO, we employ LDA+ U and a scissors correction that gives a reasonable band gap compared to experiment. We use the around mean field double-counting correction [34] and a U parameter of 5 eV for the Ni d electrons. The scissors correction is 2 eV. In the case of the NM NiO we cannot construct a good RPA screening using LDA+ U , since this approach does not open a gap in the partially filled e_g bands. Therefore we use the screening of the AFM phase also for the NM phase, such that all the calculations on NM NiO are performed in the AFM unit cell. This is a reasonable approximation since the magnetic order has little effect on the photoemission spectrum of NiO [35–37]. The lattice parameters used in this work are 4.07 Å for LiH, 5.43 Å for Si, and 8.34 Å for NiO.

In Fig. 1 we report the spectral functions of bulk LiH, Si, NM NiO, and AFM NiO. We observe that the EKT gives a large overestimation of the band gap for all these systems, but the valence part of the spectrum is well reproduced. The inclusion of screening in our SEKT equations dramatically improves the results. With the SEKT we obtained the following values for the fundamental band gap: 5.25 (4.99) eV for LiH, 1.63 (1.12) eV for Si, 1.90 (4.3) eV for NiO NM, and 2.45 (4.3) eV for NiO AFM, with the corresponding experimental gap given in parentheses [38,40]; with the EKT, instead, we obtain: 11.80 eV for LiH, 6.77 eV for Si, 17.03 eV for NiO NM, and 16.19 eV for NiO AFM.

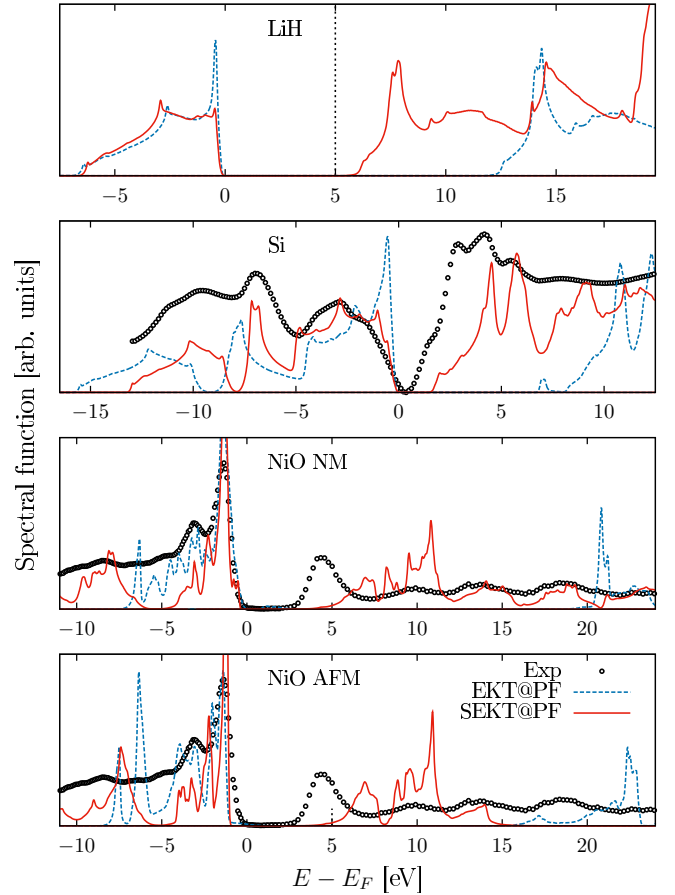


FIG. 1. Spectral function of bulk LiH, Si, NM NiO and AFM NiO: comparison of the EKT@PF and SEKT@PF. We used $\alpha = 0.65$ in the PF. Note that the SEKT@PF result for AFM NiO is plotted only up to ≈ 15 eV since we used few empty bands for computational reasons. The experimental band gap of LiH [38] is indicated with a dashed vertical line. The experimental spectra are taken from Refs. [39,40].

We observe that the introduction of the screening has no significant effect on the valence band width of LiH, while for Si we have a reduction of the bandwidth which gives a better agreement with experiments. For NiO the situation is quite different: The screening produces a stretching of the valence bands. Moreover, we observe a separation of O $2p$ and Ni d bands in the valence, as shown in Fig. 2, where the projected spectral functions of LiH, Si, NM NiO, and AFM NiO are reported. The band gap is underestimated, since Ni s states are “lowered” in energy while Ni e_g states remain too high in energy. It is interesting to analyze these two different trends: While in LiH and Si the screening introduces a kind of rigid shift of all the bands, which have predominantly s/p character, in the case of NiO it acts differently on the various bands in the band-gap region, which is a mixture of Ni s , p , d orbitals and O $2p$ orbitals. This can be explained by analyzing the two main contributions to the SEKT equations, namely, the contribution from the occupation numbers and the contribution from the Coulomb matrix elements. Fractional occupation numbers can make the second (negative) term

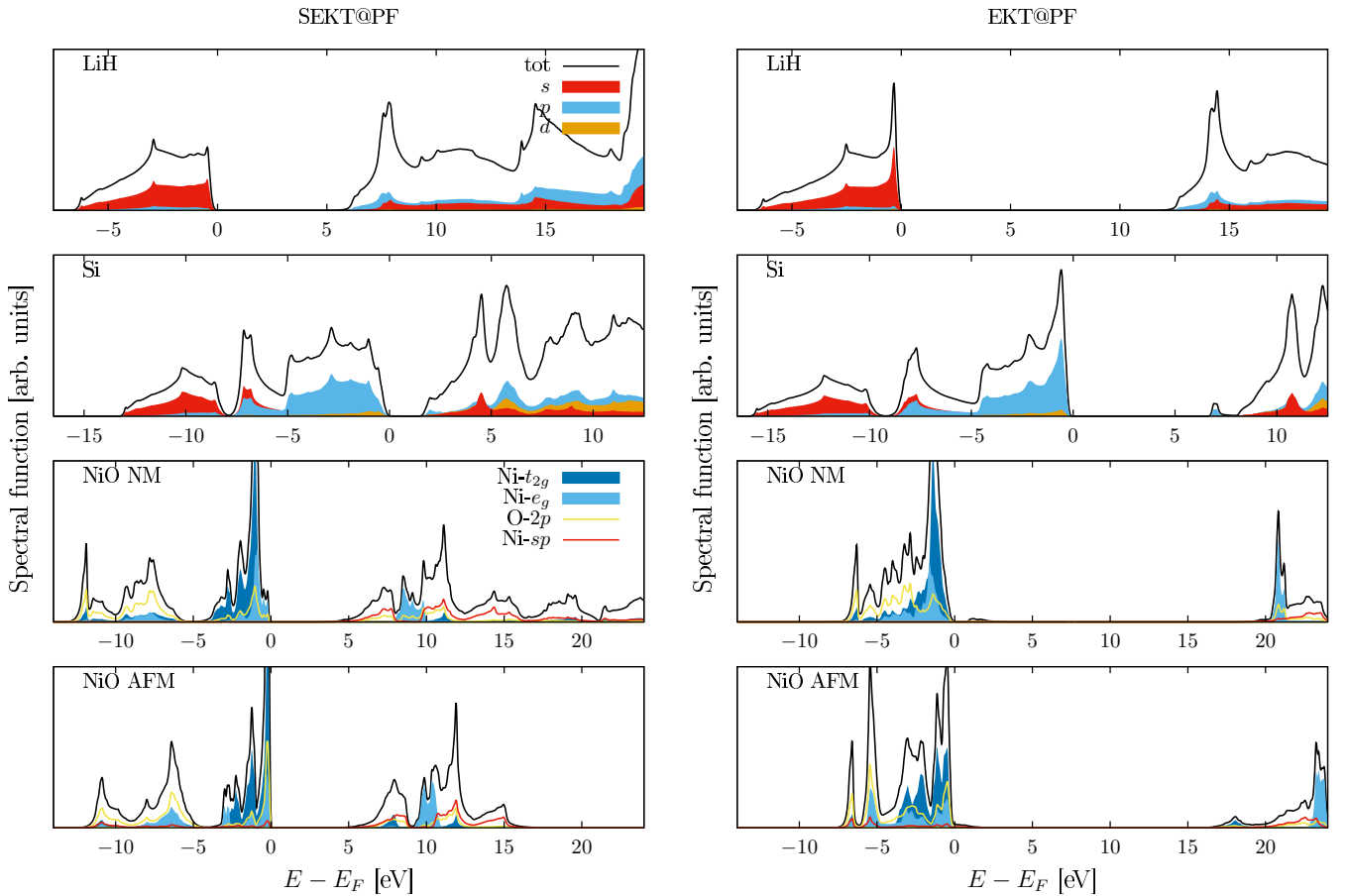


FIG. 2. Projected spectral function of bulk LiH, Si, NM NiO, and AFM NiO for the SEKT@PF and EKT@PF results. The spectral function is projected onto s , p , and d states for LiH and Si. For NiO d states are resolved into t_{2g} and e_g states.

in Eq. (3) large, which, upon application of the screening, induces a larger shift than in the case of occupation numbers close to 1. Large Coulomb matrix elements have a similar effect (one can reasonably assume that matrix elements are larger for localized states); indeed, the relative position of contributions from bands with similar occupation numbers but a different nature (e.g., localized or delocalized) change by applying the screening, which indicates the importance of Coulomb matrix elements. A similar analysis can be done for the addition energies. This suggests to improve the screening in strongly correlated materials by going beyond RPA or to introduce corrections to the SEKT based on the nature of the bands. For example, one could separate the bands into strongly occupied (occupancies larger than 0.5) and weakly occupied (occupancies smaller than 0.5) in the same spirit of the corrections proposed by Gritsenko *et al.* to remedy to the overcorrelation of the Müller functional [41] and use a different screening for these two classes of orbitals (RPA for weakly occupied and beyond RPA for strongly occupied [42]). This work is currently in progress.

As a final remark we notice that SEKT opens an unphysical band gap in the homogeneous electron gas (HEG), as shown

in the Supplemental Material [25] (See also Refs. [43,44] therein), which we expect to be closed using more advanced approximate density matrices. This also suggests to look for better approximations to the 1- and 2-RDM.

IV. CONCLUSIONS

In conclusion, we presented an approach which can describe the band-gap opening in weakly as well as strongly correlated gapped materials. Although improvements are still needed, this is a remarkable results for an *ab-initio* method and it opens the way to a unified description of photoemission spectra in weakly as well as strongly correlated systems.

ACKNOWLEDGMENTS

This study has been supported through the EUR Grant No. NanoX ANR-17-EURE-0009 in the framework of the ‘‘Programme des Investissements d’Avenir’’ and by ANR (Projects No. ANR-18-CE30-0025 and No. ANR-19-CE30-0011).

- [1] N. F. Mott, *Rev. Mod. Phys.* **40**, 677 (1968).
- [2] P. Hohenberg and W. Kohn, *Phys. Rev.* **136**, B864 (1964).
- [3] A. Fetter and J. D. Walecka, *Quantum Theory of Many-Particle Systems* (Dover, New York, 2003).
- [4] M. van Schilfgaarde, T. Kotani, and S. Faleev, *Phys. Rev. Lett.* **96**, 226402 (2006).
- [5] S. Di Sabatino, J. A. Berger, L. Reining, and P. Romaniello, *Phys. Rev. B* **94**, 155141 (2016).
- [6] P. Romaniello, S. Guyot, and L. Reining, *J. Chem. Phys.* **131**, 154111 (2009).
- [7] P. Romaniello, F. Bechstedt, and L. Reining, *Phys. Rev. B* **85**, 155131 (2012).
- [8] A. Stan, P. Romaniello, S. Rigamonti, L. Reining, and J. A. Berger, *New J. Phys.* **17**, 093045 (2015).
- [9] F. Tandetzky, J. K. Dewhurst, S. Sharma, and E. K. U. Gross, *Phys. Rev. B* **92**, 115125 (2015).
- [10] J. A. Berger, P. Romaniello, F. Tandetzky, B. S. Mendoza, C. Brouder, and L. Reining, *New J. Phys.* **16**, 113025 (2014).
- [11] M. M. Morrell, R. G. Parr, and M. Levy, *J. Chem. Phys.* **62**, 549 (1975).
- [12] D. W. Smith and O. W. Day, *J. Chem. Phys.* **62**, 113 (1975).
- [13] S. Di Sabatino, J. A. Berger, L. Reining, and P. Romaniello, *J. Chem. Phys.* **143**, 024108 (2015).
- [14] S. Di Sabatino, J. A. Berger, and P. Romaniello, *J. Chem. Theory Comput.* **15**, 5080 (2019).
- [15] S. Di Sabatino, J. Koskelo, J. A. Berger, and P. Romaniello, *Phys. Rev. Res.* **3**, 013172 (2021).
- [16] S. Di Sabatino, J. Koskelo, J. Prodhon, J. A. Berger, M. Caffarel, and P. Romaniello, *Front. Chem.* **9**, 746735 (2021).
- [17] S. Di Sabatino, J. Koskelo, J. A. Berger, and P. Romaniello, *Phys. Rev. B* **105**, 235123 (2022).
- [18] P. R. C. Kent, R. Q. Hood, M. D. Towler, R. J. Needs, and G. Rajagopal, *Phys. Rev. B* **57**, 15293 (1998).
- [19] J. Lee, F. D. Malone, M. A. Morales, and D. R. Reichman, *J. Chem. Theory Comput.* **17**, 3372 (2021).
- [20] K. Pernal and J. Cioslowski, *Chem. Phys. Lett.* **412**, 71 (2005).
- [21] P. Leiva and M. Piris, *J. Mol. Struct.: THEOCHEM* **770**, 45 (2006).
- [22] P.-O. Löwdin, *Phys. Rev.* **97**, 1474 (1955).
- [23] T. L. Gilbert, *Phys. Rev. B* **12**, 2111 (1975).
- [24] K. Pernal, and J. K. Giesbertz, in *Density-Functional Methods for Excited States*, edited by N. Ferré, M. Filatov, and M. Huix-Rotllant, Topics in Current Chemistry Vol. 368 (Springer, Cham, 2015), pp. 125–183.
- [25] See Supplemental Material at <http://link.aps.org/supplemental/10.1103/PhysRevB.107.035111> for more details on the performance of the (S)EKT with the example of bulk Si and of the HEG.
- [26] To be precise, Eqs. (1) and (2), and the corresponding spectral function, are obtained within the so-called diagonal approximation to the EKT (DEKT). We have shown that within the available approximations to the 1-RDM and 2-RDM the DEKT and EKT give essentially the same result in solids [16].
- [27] A. M. K. Müller, *Phys. Lett. A* **105**, 446 (1984).
- [28] S. Sharma, J. K. Dewhurst, N. N. Lathiotakis, and E. K. U. Gross, *Phys. Rev. B* **78**, 201103(R) (2008).
- [29] N. N. Lathiotakis, S. Sharma, J. K. Dewhurst, F. G. Eich, M. A. L. Marques, and E. K. U. Gross, *Phys. Rev. A* **79**, 040501(R) (2009).
- [30] G. Riva, T. Audinet, M. Vladař, P. Romaniello, and J. A. Berger, *SciPost Phys.* **12**, 093 (2022).
- [31] ELK, <http://elk.sourceforge.net>.
- [32] J. Heyd, G. E. Scuseria, and M. Ernzerhof, *J. Chem. Phys.* **118**, 8207 (2003).
- [33] C. Rödl, F. Fuchs, J. Furthmüller, and F. Bechstedt, *Phys. Rev. B* **79**, 235114 (2009).
- [34] F. Bultmark, F. Cricchio, O. Grånäs, and L. Nordström, *Phys. Rev. B* **80**, 035121 (2009).
- [35] O. Tjernberg, S. Söderholm, G. Chiaia, R. Girard, U. O. Karlsson, H. Nylén, and I. Lindau, *Phys. Rev. B* **54**, 10245 (1996).
- [36] I. D. Hughes, M. Däe, A. Ernst, W. Hergert, M. Lüders, J. B. Staunton, Z. Szotek, and W. M. Temmerman, *New J. Phys.* **10**, 063010 (2008).
- [37] D. Ködderitzsch, W. Hergert, W. M. Temmerman, Z. Szotek, A. Ernst, and H. Winter, *Phys. Rev. B* **66**, 064434 (2002).
- [38] M. J. van Setten, V. A. Popa, G. A. de Wijs, and G. Brocks, *Phys. Rev. B* **75**, 035204 (2007).
- [39] J. R. Chelikowsky, T. J. Wagener, J. H. Weaver, and A. Jin, *Phys. Rev. B* **40**, 9644 (1989).
- [40] G. A. Sawatzky and J. W. Allen, *Phys. Rev. Lett.* **53**, 2339 (1984).
- [41] O. Gritsenko, K. Pernal, and E. Baerends, *J. Chem. Phys.* **122**, 204102 (2005).
- [42] M. Shishkin, M. Marsman, and G. Kresse, *Phys. Rev. Lett.* **99**, 246403 (2007).
- [43] J. T. Krogel, J. Kim, and F. A. Reboredo, *Phys. Rev. B* **90**, 035125 (2014).
- [44] S. Azadi, N. D. Drummond, and W. M. C. Foulkes, *Phys. Rev. Lett.* **127**, 086401 (2021).